Sum Frequency Generation Spectroscopy and Double-Layer Capacitance Studies of the 1-Butyl-3-Methylimidazolium Dicyanamide−Platinum Interface

Cesar Aliaga and Steven Baldelli*

Department of Chemistry, University of Houston, Houston, Texas 77204

Received: June 5, 2006; In Final Form: July 25, 2006

The orientation of the cation and the anion of 1-butyl-3-methylimidazolium dicyanamide at the platinum−liquid interface, using sum frequency generation (SFG) spectroscopy is reported. Sum frequency spectra at two different polarizations and different potentials are recorded, and analysis of polarization-dependent spectra is performed to estimate the orientation of the dicyanamide anion and the alkyl and ring moieties in the cation as a function of the potential applied to the platinum electrode. In addition, cyclic voltammetry and electrochemical impedance spectroscopy are conducted. A model of the double-layer structure at the electrified interface is presented from the analysis of capacitance and SFG data.

Introduction

Room temperature ionic liquids (RTILs) are 100% ionic compounds liquid at room temperature due to weak interactions between the charged species. They are, in other words, salts in their molten state at ambient temperature. The RTILs are usually composed of an organic cation possessing low symmetry and a poorly coordinating anion, of organic or inorganic nature.[1,2] These compounds have attracted great interest because of their singular properties. They are characterized by a high conductivity, an almost complete absence of vapor pressure, a wide electrochemical window, a relatively high polarity, thermal stability, and large liquidus ranges.[2−8] Since they are composed of organic cations, a number of different ionic liquids with a broad range of unique properties can be designed. Their viscosities are usually large, on the order of a few tens of mPa·s due to the size and the association of the ions; nevertheless, some compounds exhibit relatively low viscosities and consequently relatively high conductivities, although still low compared to certain aqueous electrolytes.[1,8] Moreover, the RTILs are less corrosive than their inorganic counterparts, i.e., molten salts, and they are also outstandingly good solvents for a large variety of organic and inorganic compounds.[9−11]

Their high viscosity, however, limits their possible industrial applications as it may lead to problems in operations such as filtration, decantation, and dissolution and even to reduced reaction rates.[8] As a result of their high viscosity, their conductivity is also reduced and has values below the conductivities of some electrolytes dissolved in water, that is, on the order of 10 $m\Omega^{-1}$ cm^{-1}.[1,12] Therefore, attention has lately been focused on compounds with anions that can reduce the viscosity of the RTILs. The properties of ionic liquids based on anions such as triflate, bis(trifluoromethanesulfonyl)imide, and dicyanamide have been investigated.[3,8,9,13−15] These anions confer lower viscosities to the RTILs they form, which are on the order of ∼30 mPa·s.

Among the compounds cited above, dicyanamide-based RTILs have donor solvent characteristics and low viscosities, depending on the type of cation.[8,9] They have also been proposed as a solvent medium in dye-sensitized solar cells, yielding high efficiencies as in the work of Zakeeruddin and Gratzel.[16] Dicyanamide is itself an interesting anionic bridging ligand that can act as monodentate, bidentate, and tridentate[17] and possesses Lewis basic properties.[4]

Previous work on the metal−liquid interface of purely ionic compounds focused mainly on molten salts, which are, in their majority, inorganic salts with melting points of several hundreds of degrees Celsius. The investigation was centered mainly on differential capacity measurements as in the work of Graves,[18] Nanjundiah et al.,[19] Osteryoung et al.,[20] Devanathan et al.,[21] and Kisza.[22] Traditional inorganic salts such as alkali-metal halides were studied using either solid or liquid electrodes, and a capacitance versus potential curve was usually obtained, which showed a minimum, located at the potential of zero charge (PZC). A model of the structure of the metal−liquid interface could be derived from the capacitance measurements and from electrocapillarity measurements. It is believed that the ions close to the electrode surface are ordered in layers, where the cations alternate with the anions.

This work reports electrochemical and sum frequency generation (SFG) electrochemistry studies of the ionic liquid 1-butyl-3-methylimidazolium dicyanamide ([BMIM][DCA]), which was chosen due to its lower viscosity and the extensive research performed with the $[BMIM]^+$ cation.[6] The orientation of both the cation and the anion at the platinum−liquid interface is studied using nonlinear spectroscopy and electrochemical methods.

Previous SFG and electrochemical studies from this group focused on the same cation ($[BMIM]^+$) but with tetrafluoroborate and hexafluorophosphate anions.[23] The experiments showed that the butyl chains from the cation tend to order themselves increasingly at more positive potentials. Also, the imidazolium ring tips with respect to the surface normal, from ∼35° at positive potential to ∼60° at negative potential, although it was not possible to observe any anion vibrations due to their lower vibrational frequency, which is undetectable with the current experimental setup.

The system studied in this work is expected to provide a more complete interfacial model, based on vibrational information extracted from SFG spectra of the cation and the anion at the metal−liquid interface and from electrochemical capacitance measurements.

Structure of the Electrified Interface. The structure of the double layer at the electrode−liquid interface is important

10.1021/jp063476z CCC: $33.50
Published on Web 08/23/2006

because it influences the electron-transfer process[24] and depicts the arrangement of the ions. The structure of the electrified interface for aqueous systems has been widely studied as in the work of Grahame and others.[24,25] Different models have been proposed for the structure of the ions, such as the Helmholtz model, the Gouy−Chapman model, and the Stern modification.[26] Among the methods used to study the interface are electrocapillarity and differential capacitance (C_d), where the interface is described as a capacitor whose parallel plates are the surface of the metallic electrode and the boundary formed between the bulk liquid and the double layer. Thus, the distance between the parallel plates is equal to the double-layer thickness (d), and this can be determined with differential capacitance measurements. The simplest model is the Helmholtz description, given by[26]

$$d = \epsilon\epsilon_0/C \tag{1}$$

where d is the distance, ϵ is the relative permittivity of the medium, which has an average value of 10 for the ionic liquid,[26,27] ϵ_0 is the permittivity of free space equal to 8.85×10^{-12} F/m, and C is the capacitance (F/m^2).

Models that describe the double layer in dilute electrolytes more accurately, such as the Gouy−Chapman model and the Stern modification, have been also proposed. These take into account the variation of the capacitance with potential:[26]

$$\frac{1}{C_d} = \frac{x_2}{\epsilon\epsilon_0} + \frac{1}{\left(\frac{z\epsilon\epsilon_0 z^2 e^2 n^0}{kT}\right)^{1/2} \cosh\left(\frac{ze\phi_2}{2kT}\right)} \tag{2}$$

where C_d is the capacitance, x_2 is the distance of the outer Helmholtz plane (OHP) from the electrode surface, ϵ is the relative permittivity, ϵ_0 is the permittivity of free space, z is the charge magnitude of each ion in a z/z electrolyte, e is the electronic charge, n^0 is the number concentration of each ion in a z/z electrolyte, k is the Boltzmann constant, T is the temperature, and ϕ_2 is the potential at the OHP with respect to the bulk solution.

Another representation of the interfacial capacitance specifically derived for molten salts can be modeled by the expression (Sotnikov and Esin)[18,28]

$$\frac{1}{C_d} = \frac{1}{C_k} - \frac{4\pi\delta}{1 - 4\pi\delta\beta|\xi|} \tag{3}$$

where ξ is the charge density on the metal, $C_k = \epsilon/4\pi r$ is the capacitance of a parallel plate capacitor dependent on the permittivity of the medium ϵ with a separation equal to the radius r of the cation, and $\delta^2 = kT/[8\pi q^2 c_0(z - 2)]$ and $\beta = [8\pi\alpha q c_0(z - 1)]/kT$ are functions of the concentration of vacancies, c_0, the coordination number, z, the charge of the vacancy, q, and the polarizability, α.[18,28]

In the latter two models, the capacitance dependence on the potential applied to the electrode takes the form of a curve with a minimum located at the PZC. From the capacitance corresponding to the PZC, the thickness of the double layer can be extracted. This interpretation is formulated from a dilute electrolyte on a polarizable electrode.[26]

Sum Frequency Generation. SFG is a second-order nonlinear optical spectroscopy technique sensitive only in noncentrosymmetric environments. This makes it suitable for probing various interfaces in situ, such as gas−liquid, solid−liquid, and liquid−liquid.

In the sum frequency generation experiment, two laser beams of frequencies ω_1 and ω_2 overlap at the surface of a nonlinear medium and generate a nonlinear polarization, $\mathbf{P}^{(2)}_{(\omega 1+\omega 2)}$. The nonlinear polarization is described by

$$\mathbf{P}^{(2)} = \chi^{(2)}\mathbf{:EE} \tag{4}$$

where $\mathbf{E}$ is the electric field of the incoming laser beam and $\chi^{(2)}$ is the second-order nonlinear susceptibility, a third-rank tensor. The intensity of the SFG signal (I_{SF}) is defined as the square of the absolute value of the nonlinear polarization.

The susceptibility itself has nonresonant and resonant terms, χ_{NR} and $\sum\chi_R^{(2)}$, respectively. The former is a background effect from the interface, and $\sum\chi_R^{(2)}$ includes contributions from individual resonant modes $\chi_R^{(2)}$ that can be expressed as $\chi_R^{(2)} = N\langle\beta^{(2)}\rangle$, where N is the number of modes contributing to the SFG signal and $\beta^{(2)}$ is the molecular hyperpolarizability which contains the Raman polarizability and the IR dipole transition moment averaged over the molecule orientations. The susceptibility can be expressed as

$$|\chi^{(2)}|^2 = |\chi_{NR}{}^{(2)} + \sum\chi_R{}^{(2)}|^2 = \left|\chi_{NR}{}^{(2)} + \sum\left(\frac{A_q}{\omega_{IR} - \omega_q + i\Gamma_q}\right)\right|^2 \tag{5}$$

where A_q is the amplitude of the resonance of the qth vibrational mode, Γ_q is the damping constant for the qth vibrational mode, ω_q is the molecule normal mode of vibration, and ω_{IR} is the frequency of the incoming IR beam. It is evident that whenever ω_q becomes comparable to ω_{IR}, $\chi_R^{(2)}$ becomes large, resulting in a feature in the SFG spectrum.[29−32]

Experimental Section

Materials. The ionic liquid used in this investigation was synthesized according to literature methods.[4,8,33] 1-Chlorobutane, 99%, 1-methylimidazole, redistilled, 99+%, ethyl acetate, anhydrous, 99.8%, silver nitrate, >99%, methanol, 98%, and activated charcoal were purchased from Aldrich, sodium dicyanamide, 96%, was obtained from Alfa Aesar, and all were used without further purification. The water was deionized using a Millipore A10 system and has a resistivity of 18 MΩ cm and a TOC index of <3 ppb.

Sample Synthesis. 1-Butyl-3-methylimidazolium was synthesized by mixing 1-methylimidazole with 1-chlorobutane in a 1:1.1 molar ratio and the mixture refluxed under inert gas at a temperature of 65 °C for 72 h. The resulting 1-butyl-3-methylimidazolium chloride ([BMIM][Cl]) was then washed three times with ethyl acetate and then dried under vacuum.

Silver dicyanamide was prepared by reacting sodium dicyanamide with silver nitrate and washing the precipitate [Ag(N(CN)$_2$)] several times until no ionic silver was detected as AgCl precipitate in the washing liquid using a dilute NaCl solution. This freshly prepared solid was added to a solution in water of ([BMIM][Cl]), and the mixture was stirred for 3 h to form [BMIM][DCA]. The precipitate (AgCl) was filtered off and the water removed by rotary evaporation. The resultant liquid was dissolved in methanol and refrigerated for several hours to precipitate any silver dicyanamide left, which was filtered off, and the solvent was removed again by rotary evaporation. The sample was then dissolved in methanol, treated with activated charcoal for approximately 4 h, and filtered. Finally, it was passed through a silica gel column over a period of 10 h and filtered through a glass frit, before it was preliminarily dried in a rotary evaporator and finally dried in a

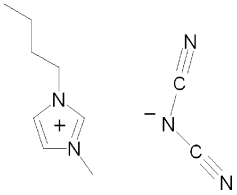

Figure 1. Scheme of the structure of the ionic liquid [BMIM][DCA].

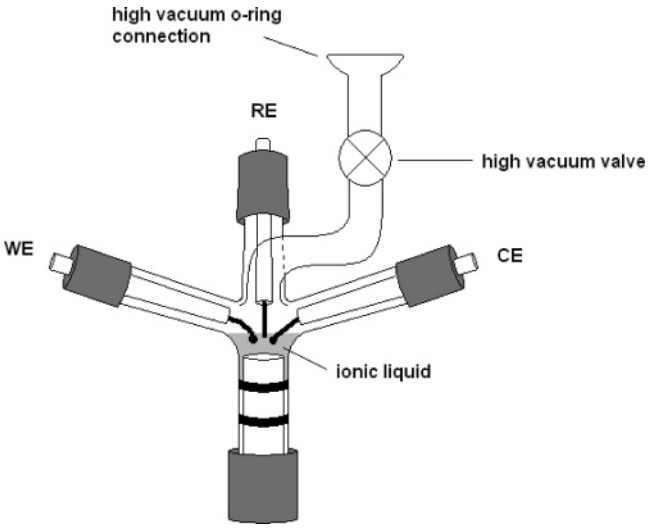

Figure 2. Scheme of the electrochemical cell showing the four arms and the working (WE), counter (CE), and reference (RE) electrodes. The high-vacuum connection, which is attached to the top of the convergence point of the three upper arms, has a high-vacuum stopcock valve and ends in an O-ring joint.

vacuum line to a pressure of 5×10^{-5} Torr. The final product is a clear and nearly colorless liquid. The samples were then characterized by nuclear magnetic resonance using a GE QE-300MHz and their electrochemical window and purity tested by cyclic voltammetry (CV) using a Pine potentiostat [AFCBP1]. The structure of [BMIM][DCA] is shown in Figure 1.

Sample Preparation for Capacitance and Cyclic Voltammetry Measurements. The Pyrex electrochemical cell used for this experiment was built in this laboratory and comprises four arms, three ending in compression fittings and the fourth containing a Teflon stopcock coupled to a reverse thread. A diagram of the cell is presented in Figure 2. All the materials inside the cell that come into contact with the ionic liquid are chemically inert. The working, counter, and reference electrodes are made of platinum. In electrochemical research in ionic liquids, metallic silver is commonly used as the reference electrode due to the fact that traditional reference electrodes may contaminate the sample with ions or water. In this investigation, platinum metal was used instead, because the Ag electrode dissolves in [BMIM]-[DCA] when a potential is applied.

The Pyrex section of the cell was cleaned and baked at 570 °C, the stopcock was boiled in Micro 90 or Alconox and then boiled several times in deionized water, and the electrodes were cleaned in concentrated nitric acid for several hours and finally thoroughly rinsed with water. The electrodes are made of corrosion-resistant stainless steel, to which platinum wire has been soldered. They were positioned in such a way that only the platinum metal was in contact with the solution.

Before the measurement, approximately 1 mL of dry sample was introduced into the cell using a clean glass pipet, with the stopcock lowered, so that the liquid was not in contact with the electrodes. Following that, the working electrode was flame annealed in an air−hydrogen flame for 5 min and immediately

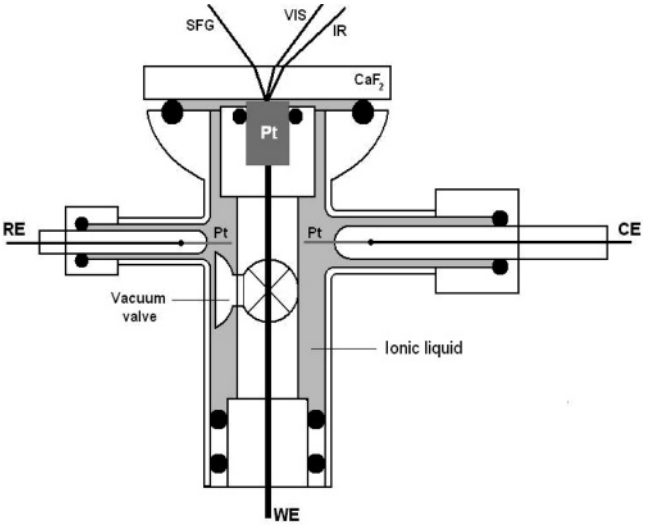

Figure 3. Schematic of the SFG electrochemical cell. The two laser beams overlap at the surface of the polycrystalline platinum working electrode, which is tightly pressed against the window (shown at the center). The counter and reference electrodes as well as the CaF_2 window and the central shaft are sealed with Kalrez O-rings (shown as dark disks) to the body of the cell. The ionic liquid fills the lightly shaded areas of the plot.

introduced into the cell, which was being purged with argon, to cool it. Finally, the Teflon stopcock was raised so that the surface of the liquid came in contact with the electrodes, and the cell was attached to a liquid nitrogen trapped vacuum line and pumped until the pressure reached 10^{-5} Torr.

Sample Preparation for the Calibration of the Platinum Quasi-Reference Electrode. The calibration of the platinum reference electrode was performed using ferrocene (biscyclopentadienyliron), symbolized Fc, whose redox potential is often used as a common standard.[34−36] It was found that ferrocene is easily dissolved in [BMIM][DCA], thus facilitating the manipulation.

The experiment was carried out in a compartmentalized electrochemical cell, with an Fc concentration of 1×10^{-3} mol/L in ionic liquid, using platinum reference, counter, and working electrodes. The ionic liquid sample was previously dried with the same procedure used for the capacitance measurements, and a weighed amount of Fc was added by opening a valve that connects both compartments. Following the dissolution of the standard, a cyclic voltammogram was taken at a scan rate of 100 mV s^{-1}. All the reported values in this work are relative to the Ag quasi-reference electrode.

Sample Preparation for the SFG Experiment. The Pyrex SFG electrochemical cell that contains the sample was built in this laboratory (Figure 3). The body is cylindrical and ends in an O-ring fitting, to which a calcium fluoride window is attached and sealed with a Kalrez O-ring. The other end is a compression fitting which holds a Kel-F shaft that seals against the inner walls of the cell with Kalrez O-rings. The working electrode is attached to the shaft using a Teflon compression fitting. The shaft can be moved along the cylindrical axis using a cap with a reverse thread, in such a way that the electrode is pressed against the calcium fluoride window. The cell has four additional connections. Two of those are O-ring-fitting-terminated high-vacuum valves, which are used to evacuate and fill the cell with the sample. The remaining two are compression fittings that accommodate the counter electrode and the quasi-reference electrode. All the materials that come in contact with the ionic liquid are chemically inert (platinum, Teflon, Kel-F, Kalrez). The cell is able to hold a vacuum down to a pressure of 10^{-6} Torr.

The working electrode (WE), counter electrode (CE), and reference electrode (RE) are made of platinum. The latter two are made of 1 mm diameter platinum wire sealed to a $^1/_4$ in. soda glass tube. The former is a 1 cm high, $^1/_4$ in. diameter polycrystalline platinum cylinder on which one of the faces was polished with successively finer grades of diamond powder and finally alumina powder down to 0.05 μm, until a mirror-like appearance was obtained. The visible 532 nm and the tunable IR beams overlap at the surface of this electrode, and the sum frequency signal is generated.

Before introduction of the sample into the cell, the glass body was cleaned in a 50/50 nitric acid/sulfuric acid mixture, rinsed with deionized water, and baked at 570 °C. The reference and counter electrodes were cleaned in the acid mixture and then rinsed thoroughly with water. The calcium fluoride was repeatedly rinsed with water and finally cleaned with spectrophotometric grade methanol using lens cleaning wipes. The remaining parts of the cell were boiled in water plus Micro 90 or Alconox detergent and finally boiled again several times in deionized water. The working electrode was rinsed in water, flame annealed in an air−hydrogen flame for 5 min, and cooled in an argon atmosphere, following a procedure similar to the Clavilier method.[37] Following that, a drop of the ionic liquid to be tested was added to its polished surface to prevent any impurity adsorption, and it was finally assembled with the rest of the parts. The completed cell was then immediately connected to the vacuum line and dried until a pressure of 5×10^{-5} Torr was reached.

The ionic liquid sample was dried in a separate vessel equipped with an O-ring fitting. Once the desired pressure was reached, the vessel was pressurized with dry argon, and the ionic liquid was airless transferred to the SFG cell. The compound was thus never exposed to the atmosphere. A cyclic voltammogram was obtained using an AFCBP1 Pine potentiostat and then the electrode was tightly pressed against the window before the cell was taken to the spectroscopy setup, where sum frequency spectra were taken at different potentials.

Finally, to discriminate between the signal generated at the liquid−electrode interface and the potential signal generated at the liquid−CaF_2 interface, a preliminary experiment was carried out. It consised of filling the cell with the ionic liquid sample as described above and acquiring the spectra at different polarizations, at open circuit, with the electrode pulled away from the CaF_2 window approximately 1 mm, and with the laser at full power intensity. This allows for probing the liquid/calcium fluoride interface alone. Once the spectra of the latter interface is taken, it can be used to discriminate between the two different sources of signal in the final spectra, since the features of that interface are not supposed to be affected by the potential as opposed to the features generated at the platinum interface.

Spectroscopy System. The spectroscopy setup consists of an EKSPLA PL2143A/20 picosecond pulsed Nd:YAG laser with a 25 ps pulse and a 20 Hz repetition rate, whose 1064 nm output pumps an optical parametric generation/amplification system (LaserVision OPG/OPA). The OPG/OPA system produces an infrared beam tunable from 2000 to 4000 cm^{-1} using two nonlinear crystals: $KTiOPO_4$ and $KTiOAsO_4$. It also doubles the frequency of the 1064 nm beam to produce a 532 nm beam using a $KTiOAsO_4$ crystal. The fixed visible and the tunable infrared beams are collimated and overlap at the surface of the liquid following a copropagating geometry, with angles (with respect to the surface normal) of 50° for the visible and 60° for the IR. The infrared beam is focused a few centimeters beyond the sample surface using a +150 mm IR lens, while the 532 nm beam is focused and collimated using a simple telescope formed by a +200 mm lens followed by a −75 mm lens. The beam areas at the surface are 0.5 mm^2 for the infrared beam and 1.99 mm^2 for the 532 nm beam. The energies per pulse for the infrared beam at the two vibrational ranges studied are 5.1 mJ (C−H stretch range) and 2.1 mJ (C≡N stretch range), and the energy per pulse for the 532 nm beam is 8.11 mJ. These pulse energies yield energy densities at the surface of the sample of 20.4 mJ/cm^2 for the 532 nm beam and 55.43 and 22.47 mJ/cm^2 for the infrared beam at 2879 and 2100 cm^{-1}, respectively. The SFG signal reflected from the surface is filtered with a 515 nm short-pass filter and a monochromator and collected by a photomultiplier tube (Hamamatsu R3788). The signal is then sent to a gated integrator, and a computer program collects it and averages it over 5 or 10 scans of 20 shots/point at 1 cm^{-1}/s. The polarization of the incoming and SFG beams is changed using a waveplate ($\lambda/2$) and Glan-Laser polarizers. The polarization combinations used are ssp and ppp, "s" and "p" meaning electric field vector perpendicular and parallel to the plane of incidence, respectively. The first, second, and third letters correspond to the polarization of the sum frequency, green, and infrared beams, respectively.

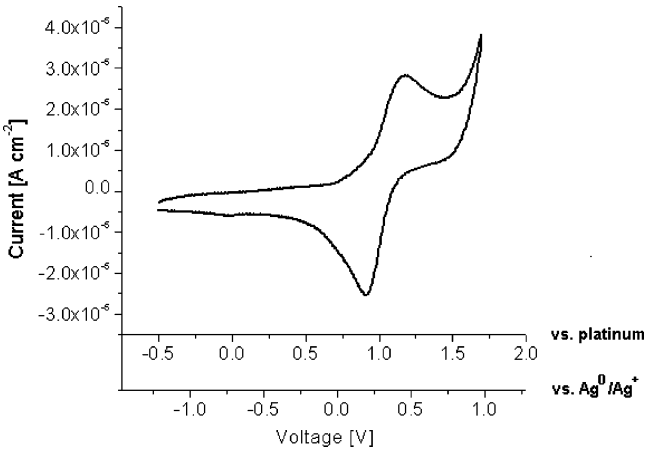

Figure 4. Cyclic voltammetry of ferrocene (1×10^{-3} M) in [BMIM][DCA] at a platinum electrode. Potentials are shown vs a Pt quasi-reference electrode and versus a Ag^0/Ag^+ quasi-reference electrode.

Data Collection and Analysis. The frequency of the IR laser beam was scanned at a rate of 1 cm^{-1}/s. After collection of 20 shots, these were averaged, and 1 data point was plotted on the screen. Five spectra per polarization combination were obtained, and the average was plotted along with error bars that represent the standard deviation between them. The data were corrected for fluctuations in the infrared beam by dividing the averaged spectrum by data collected in the reference channel to account for any absorption from the liquid phase. The spectra were then fitted using the program Origin 6.0 and eq 5, using a nonlinear fitting algorithm, in which the line shape of the peaks is modeled using Lorentzian functions. The fitting was carried out using instrumental setting to take into consideration the error due to the scattering of the experimental points.

Results

Electrochemical Characterization. The cyclic voltammetry of the ferrocene−ionic liquid solution is shown in Figure 4, using a spherical platinum working electrode of an area of 0.22 cm^2, with a scan rate of 100 mV s^{-1}. The reduction peak of ferrocene is located at +0.9 V. Bibliographic data show that the reduction potential of ferrocene dissolved in the ionic liquid [BMIM][PF_6], relative to the cobaltocenium cation ([$Co(Cp)_2$]$^+$), is +1335 mV, whereas the latter has a reduction potential of −1145 mV relative to silver.[34,35] Using those considerations, it

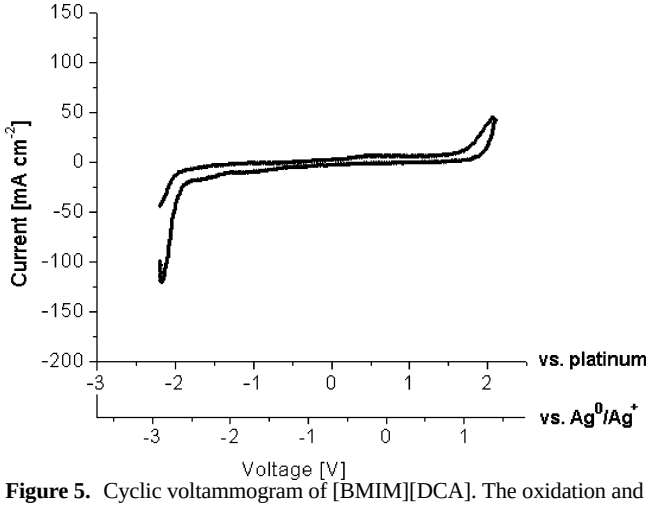

Figure 5. Cyclic voltammogram of [BMIM][DCA]. The oxidation and reduction onsets start at aproximately 2 and −2 V, respectively (versus a platinum quasi-reference electrode), giving an electrochemical window of ca. 4 V.

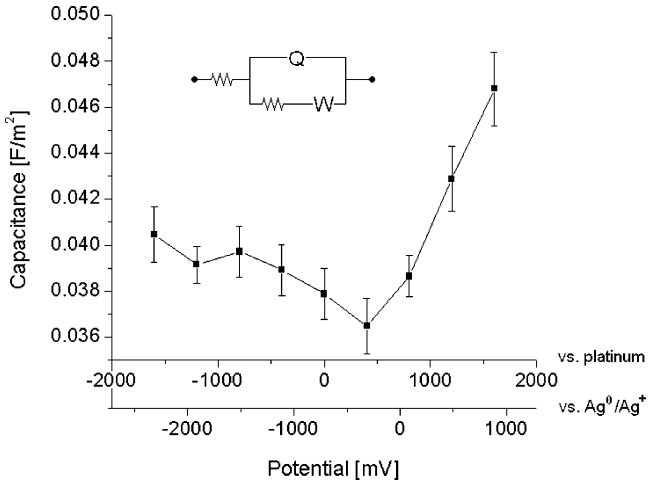

Figure 6. Capacitance versus potential plot at the [BMIM][DCA]−platinum interface. The potential of zero charge corresponds to the minimum of the curve depicted by the experimental points and is located approximately at 600 mV versus a platinum quasi-reference electrode or −115 mV versus a Ag^0/Ag^+ quasi-reference electrode. The equivalent circuit R(Q(RW)) used to extract the capacitance from the impedance data is shown at the top.

is found that the reduction potential of ferrocene relative to silver is +187 mV.

The cyclic voltammetry of [BMIM][DCA] is shown in Figure 5 using the same working electrode as in the previous test and a scan rate of 100 mV s^{-1}. The plot shows an electrochemical window of approximately 4 V, being stable down to −2 V and up to +2 V, after performance of the calibration. This value is similar to that reported by MacFarlane et al., who found a window of 3.5 V. It is believed that, beyond the maximum positive potential, an irreversible oxidation occurs which generates a neutral dimer, $[N(CN)_2]_2$.[4,8]

To probe the double-layer structure, EIS was performed at potentials ranging from −1600 to +1600 mV in 400 mV intervals. The $-Z$ imaginary vs $+Z$ real data were then fitted with ZsimpWin v.2 software, using an R(Q(RW)) circuit as the equivalent, where a constant phase element "Q" was used instead of a double-layer capacitor to obtain acceptable fitting results. The capacitance data were then extracted from the value of the constant-phase element using the formula given by Hsu and Mansfeld:[38] $C = Q(2\pi f_{max})^{n-1}$. Here, f_{max} is the frequency at which the imaginary part of the impedance has a maximum in an R(QR) loop simulated using the fitting data of the corresponding Nyquist plot and n is the power of the constant-phase element obtained from the fitting, which yielded an average value of 0.91. The differential capacitance versus potential curve for the [BMIM][DCA]−platinum interface is shown in Figure 6 (the diagram of the R(Q(RW)) circuit is shown as an inset). The potential of zero charge, which corresponds to the minimum of the curve,[18,26] is approximately −315 mV versus silver. This value falls in the range of several ionic liquids.[19] The capacitance corresponding to the PZC is 0.037 F/m^2, which can be used to estimate the thickness of the double layer. The Helmholtz, Gouy−Chapman−Stern, and Sotnikov and Esin's models were used to estimate the thickness.[18,26,28,39] In this case, all the approaches yield a double-layer thickness of approximately 25 Å. A plot of charge versus voltage is also shown in Figure 7.

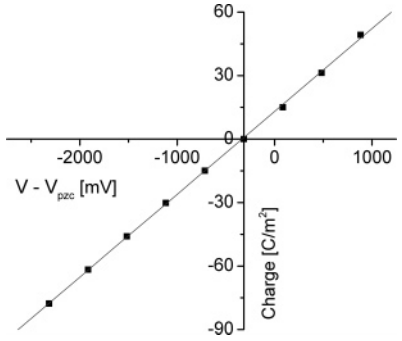

Figure 7. Charge versus potential plot at the [BMIM][DCA]−platinum interface. The data follow a linear trend.

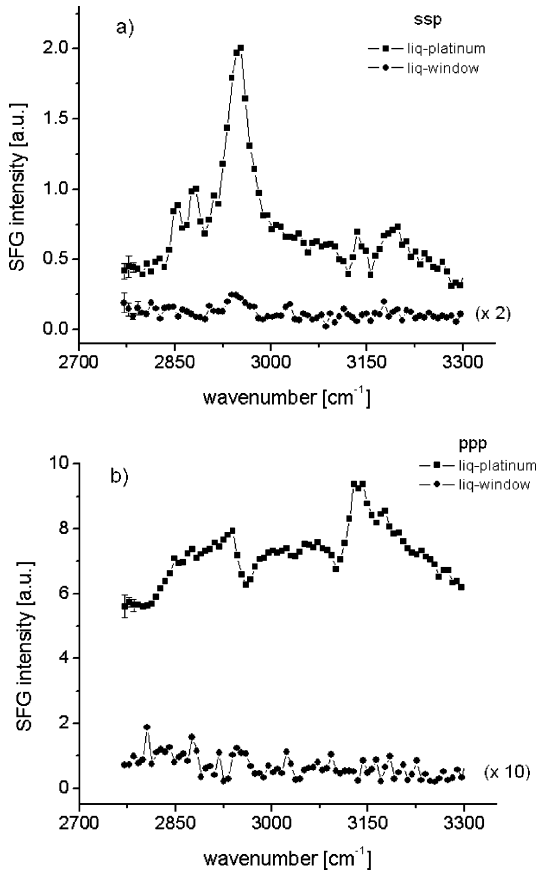

Figure 8. Comparison of sum frequency generation spectra at two different liquid−solid interfaces. (a) and (b) show the C−H stretching region for ssp and ppp polarization combinations. The spectra generated at the platinum−liquid interface (squares) have more resonant background and show stronger peaks than the spectra from the CaF_2−liquid interface (circles), which are shown on different scales.

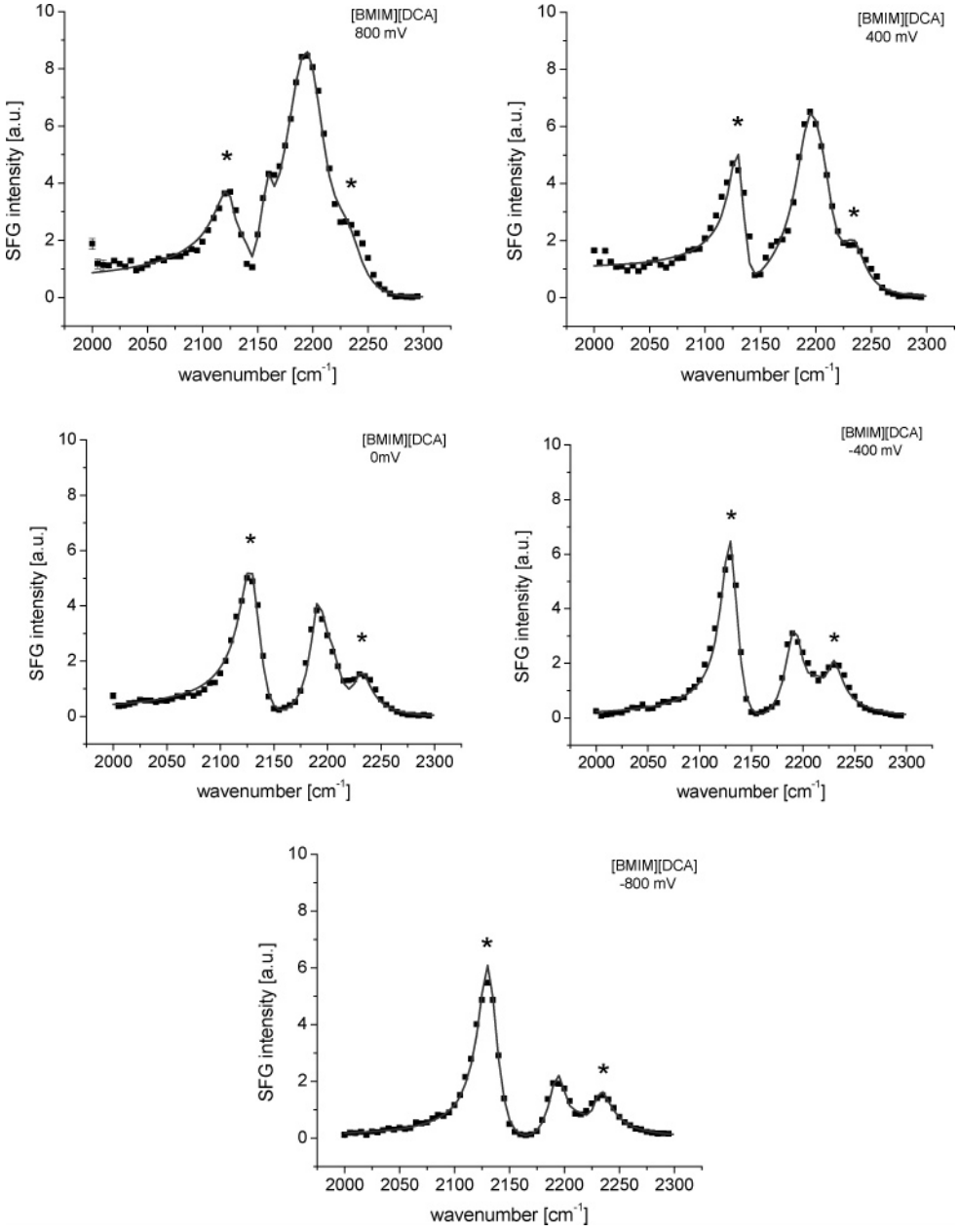

Figure 9. Potential-dependent SFG spectra of [BMIM][DCA] at the liquid−Pt interface in the ssp polarization combination for the C≡N stretch region at different potentials. The asterisks over the peaks point to the signal generated at the CaF_2 window.

The linear trend of the data was obtained after integration of the area under the curve of capacitance versus potential for voltages positive relative to the PZC.

Spectroscopy. The 2000−2300 cm^{-1} frequency interval for the anion (C≡N stretch vibrational modes) and the 2750−3300 cm^{-1} interval for the cation (C−H stretch vibrational modes) were chosen for the sum frequency spectroscopy.

The spectra of the liquid−calcium fluoride interface for the C≡N stretch region in ssp and ppp (not shown) displayed vibrations that correspond to the antisymmetric C≡N stretch at ∼2130 cm^{-1}, the symmetric stretch at ∼2190 cm^{-1}, and a combination band between the antisymmetric and symmetric N−C stretches at ∼2230 cm^{-1}.[40,41] Additional spectra (also not shown) were taken at different voltages to determine any changes with potential, which would signify that the signal comes from the metal−liquid boundary. No changes were observed.

Spectra in the CH stretch region for the liquid−calcium fluoride interface were also recorded and are plotted in Figure 8. Spectra at the liquid−platinum interface are shown for comparison. The signal intensity from the CaF_2−liquid interface is negligible compared to the platinum−liquid boundary signal for the CH stretch region, as shown in the plots.

The spectra of [BMIM][DCA] for polarizations ssp and ppp in the C≡N stretch region are shown in Figures 9 and 10 for the potentials of −800, −400, 0, 400, and 800 mV. The features at 2130 and 2180 cm^{-1} correspond to the antisymmetric and the symmetric C≡N stretches, respectively. The vibrations that contain the contribution from the window are marked with asterisks. The feature at 2230 cm^{-1} is a combination band of the symmetric and antisymmetric N−C stretching modes.[40,41] The analysis of the fitting of the data yields ranges in which the assigned peaks vary with potential in the ranges of 2126−2132 cm^{-1} for the antisymmetric C≡N stretch, 2192−2205 cm^{-1} for the symmetric C≡N stretch, and 2228−2253 cm^{-1} for the combination band. The plots in the ssp polarization combination show a dramatic increase in the amplitude of the antisymmetric C≡N stretch, with an increase in potential,

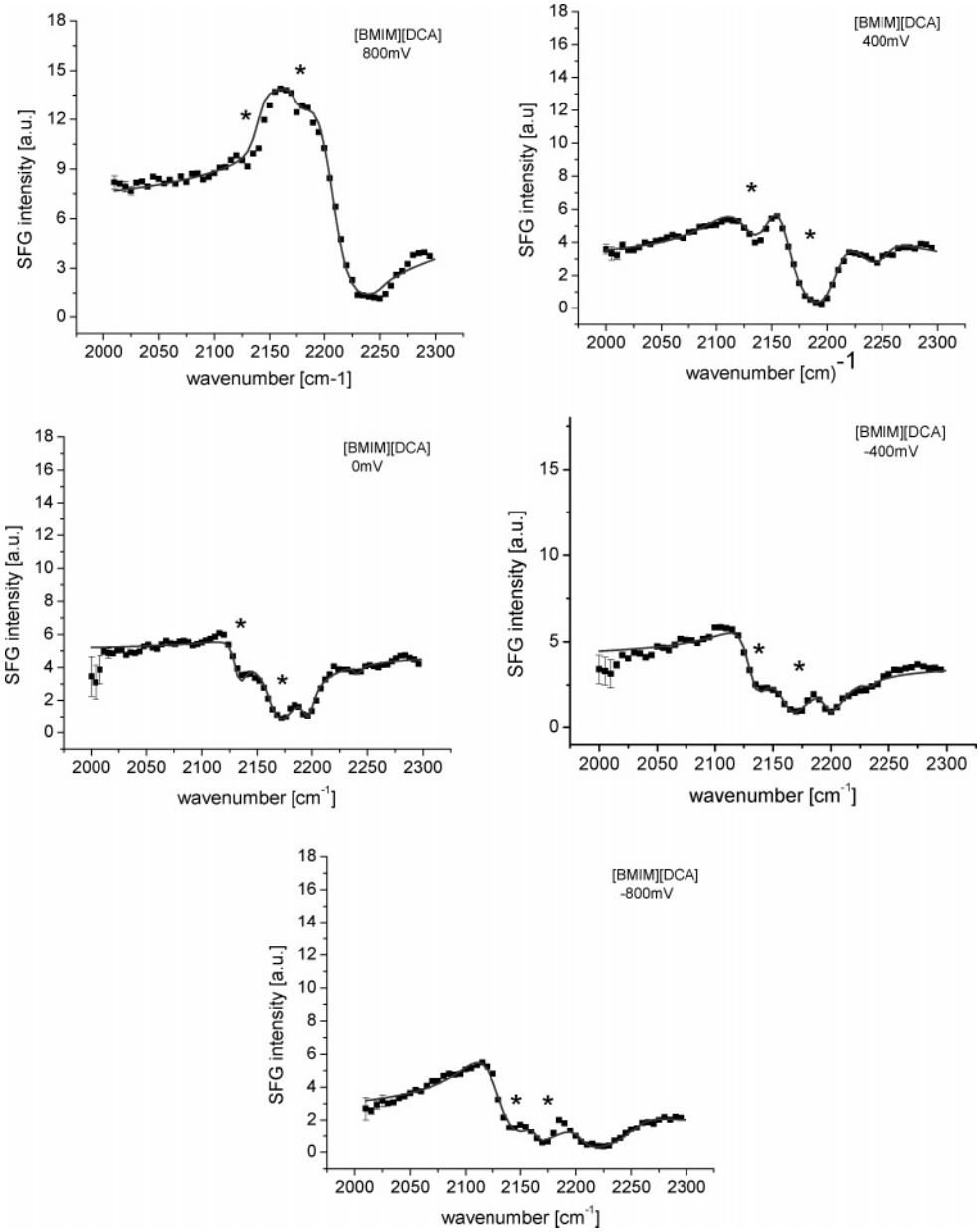

Figure 10. Potential-dependent SFG spectra of [BMIM][DCA] at the liquid−Pt interface in the ppp polarization combination for the C≡N stretch region at different potentials. The asterisks over the dips point to the signal generated at the CaF_2 window.

whereas the amplitude of the antisymmetric C≡N stretch decreases. In the ppp spectra the vibrational frequencies appear as dips, and the main change due to the increase in applied potential is an increment in the background signal, as well as in the amplitude of the 2180 cm^{-1} dip.

The C−H stretching region is shown in Figures 11 and 12. The ssp and ppp combinations contain the symmetric (d^+) and antisymmetric (d^-) methylene stretches at 2850 and 2910 cm^{-1}, respectively, and the symmetric (r^+) methyl stretch and its Fermi resonance (r^+_{FR}) at 2879 and 2940 cm^{-1}, respectively.[42−44] There is a broad and weak feature (hydrogen bond) at 3040 cm^{-1} that corresponds to the hydrogen-bonding interactions, and the C_4-C_5 ring vibrations are located at 3150 and 3190 cm^{-1} for the antisymmetric and the symmetric vibrations, respectively.[45−47] The fitted peak ranges are 2910−2916 cm^{-1} for d^-, 2847−2961 cm^{-1} for d^+, 2871−2886 cm^{-1} for r^+, 2935−2952 cm^{-1} for r^+_{FR}, 3030−3045 cm^{-1} for the H-bond, 3137−3148 cm^{-1} for the C_4-C_5 antisymmetric vibration, and 3178−3213 cm^{-1} for the C_4-C_5 symmetric vibration. The 2910 and 3040 cm^{-1} peaks are only visible in ppp, which has a strong nonresonant background, and is the only combination that shows all seven vibrational modes cited above.

In the ssp polarization combination, as the potential turns positive, the amplitude of the peak corresponding to the symmetric C_4-C_5 ring vibration increases in intensity, whereas the amplitudes from the methylene symmetric and antisymmetric vibrations (barely visible as shoulders close to the 2940 cm^{-1} peak only at −800 and −400 mV) show the opposite behavior. The ppp polarization combination shows a diminution in the amplitudes of the ring modes and an intensification of the nonresonant background when the potential increases. The spectra share similar features with previous results for ionic liquids in experiments performed in this laboratory.[23]

Discussion

Information on the orientation of the molecules at the liquid−platinum interface can be obtained through the analysis of polarization-dependent SFG spectra as approximation of the tilt angles from the surface normal. In addition, the structure of the electrochemical double layer can be addressed through

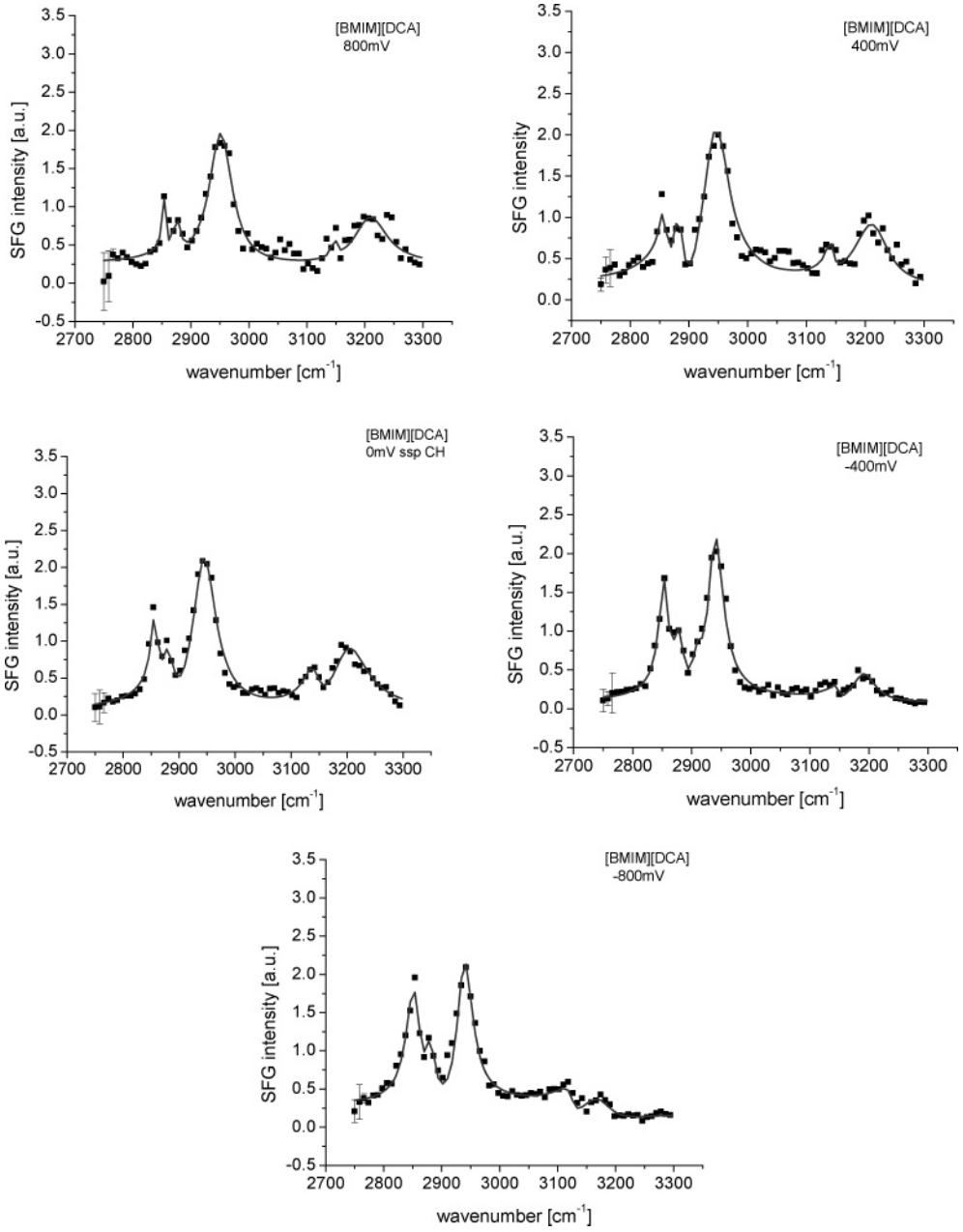

Figure 11. Potential-dependent SFG spectra of [BMIM][DCA] at the liquid−Pt interface in the ssp polarization combination for the C−H stretch region at different potentials.

differential capacity measurements in the metal−liquid interface employing electrochemical impedance spectroscopy.

Electrochemistry. The electrochemical results provide useful insight into the structure at the interface. The thickness of the double layer extracted from the curve of the capacitance versus potential, seen in Figure 6, was calculated to be approximately 25 Å with three different electrochemical models as described above. Interestingly, the Helmholtz and Gouy−Chapman−Stern descriptions wherein the latter is derived for electrolytic solutions yield results similar to those of the Sotnikov and Esin model, which was devised for molten salts. Furthermore, the latter two models reduce to a simple Helmholtz description, as the second term in each of eqs 2 and 3, corresponding to the "diffuse double layer", becomes negligible compared with the first term, which corresponds to the capacitance of the double layer. It is important to state that the value of 10 chosen for the dielectric constant ϵ of the ionic liquid near the electrode corresponds to the bulk value. Some discussions in the literature show that the value of ϵ for water substantially decreases as the distance from the electrode diminishes to values near the molecular dimensions, due to the influence of the electric field on the water dipole.[48] Due to the lack of studies on the dielectric constant values for ionic liquids near electrodes, the effect of the electric field on the charged ions is unclear. However, a smaller value of ϵ would cause the double-layer thickness to be smaller; thus, the double-layer thickness reported here (25 Å) is an upper limit value. Previous studies used a value of $\epsilon = 7$ to estimate the double-layer thickness and gave a value consistent with Stark shift measurements.[23,49]

Taking into account that the dimensions of the ions investigated fall in the range of 2−10 Å,[50,51] these results suggest that a multilayer of adsorbed ions exists at the surface of the electrode. The results obtained from the calculation of the double-layer thickness lead to the idea that the multilayer possesses a simple Helmholtz-type structure, which postulates that the excess charge of the metallic phase and the solution reside at the interface, thus creating two planes of charge of opposite sign. The multilayer of ions differs from an insulating

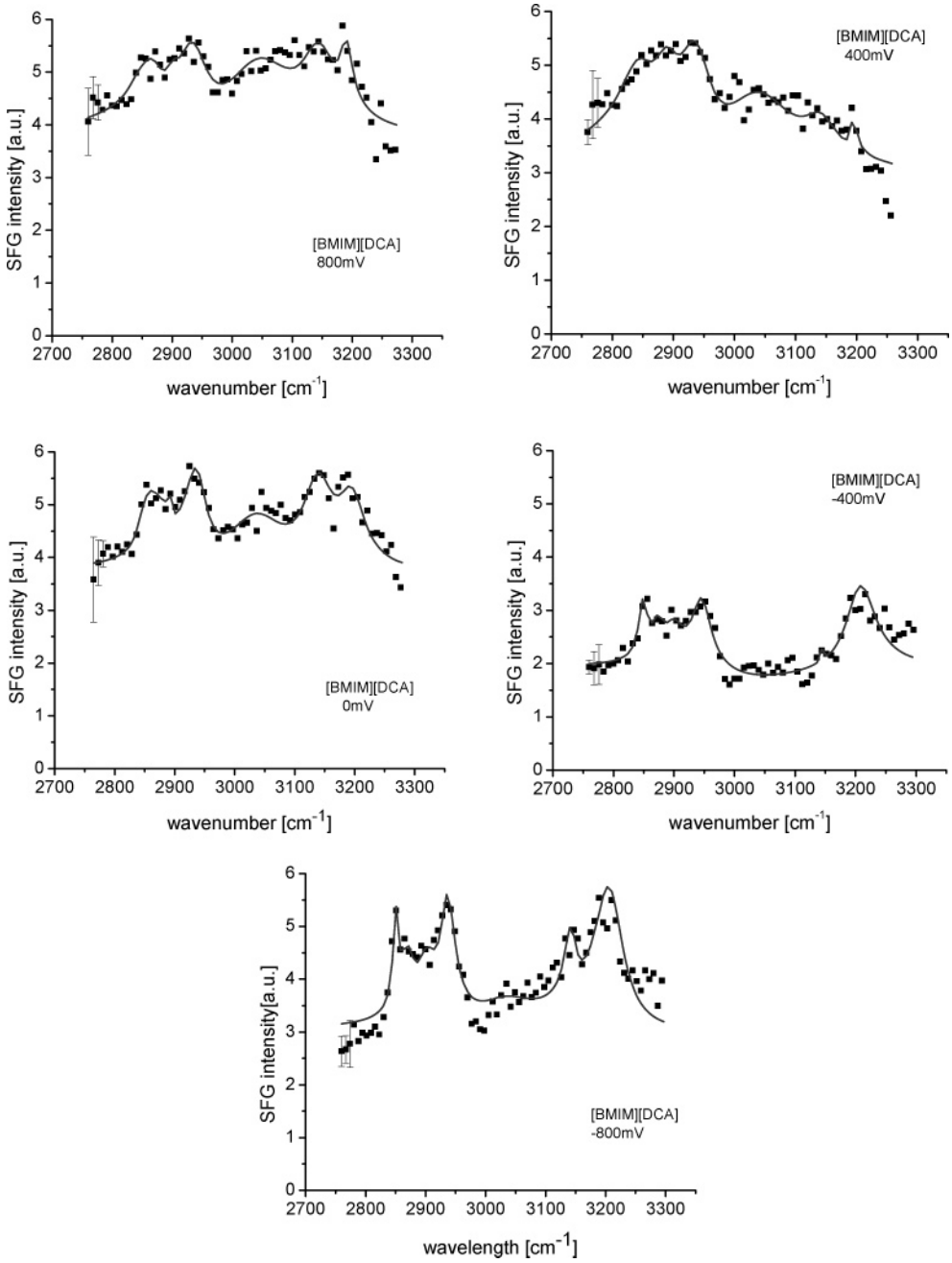

Figure 12. Potential-dependent SFG spectra of [BMIM][DCA] at the liquid−Pt interface in the ppp polarization combination for the C−H stretch region at different potentials.

layer grown at the electrode surface because no current was detected in the cyclic voltammogram (Figure 5) inside the electrochemical window, implying that no electrochemical reaction took place. These results are similar to those of Lipkowsky et al., where capacitances of comparable order of magnitude were found for multilayers of 12-(9-anthroyloxy) acid adsorbed on a gold(111) electrode.[52] Comparable results are those from the work of Sotiropoulos et al.[53] for multilayers of oleate that generated capacitances of the same order of magnitude as in this work; additionally, Tadjeddine et al.[54] reported the formation of bilayers of cyanide and thiocyanate on a platinum surface by electrochemical adsorption. However, the results differ from those of previous spectroscopic and electrochemical experiments performed with 1-butyl-3-methylimidazolium tetrafluoroborate. In those results, the ions adsorbed at the surface of a platinum electrode formed a Helmholtz-type layer one ion thick.[49] This difference likely arises from the presence of cyanide moieties in dicyanamide, which adsorb strongly to the platinum surface.[54−56]

In the present work, a vibrational Stark effect was expected, but the results showed virtually no Stark shift, which may be due to an electric field of lower intensity at the surface of the metal and a lower inherent Stark shift of cyano groups compared to CO. Moreover, the cyano moieties of the anion are not believed to be oriented along the surface normal since the C_2 symmetry axis is nearly parallel to the surface normal.

Spectroscopy. For the orientation analysis of the SFG spectra, the following assumptions are made: The terminal methyl groups of the alkyl chains of the cation are assigned C_{3v} symmetry. Both the C_4-C_5 group of the cation and the dicyanamide anion are assumed to possess C_{2v} symmetry; however, only the latter is considered to possess a free rotation about the C_2 axis.

The SFG spectra for the C≡N stretching region show a strong signal intensity. At the ssp polarization combination it was

observed that, as the potential goes from negative to positive values with respect to the PZC, the intensity of the symmetric stretch peak at 2190 cm^{-1} increases. It is known that the SFG intensity is proportional to the concentration and ordering of the species.[30,31] Therefore, the incremental increase in the intensity of the symmetric stretch peak suggests two possible contributions. The first one is that the C_2 symmetry axis of the dicyanamide anion tends to align itself parallel to the surface normal with an increase of the potential, thus increasing the ordering of the molecules. This is similar to the work of Daum et al. on cyanide adsorption on platinum electrodes in aqueous solutions, which shows that the ion adsorbs with its symmetry axis perpendicular to the surface and that the tilt away from the surface normal decreases with the increase in the potential.[55] Somorjai et al. also showed a similar tendency of the cyano group to adsorb with its symmetry axis perpendicular to the surface.[37,57]

The other possible contribution to the strength of the signal comes from an increase of the concentration of dicyanamide ions at the surface of the platinum electrode, as the surface charge becomes positive with respect to the PZC. This seems due to the tendency of dicyanamide to strongly adsorb to certain metals. In the literature, different nitrogen-containing compounds were probed in reference to their behavior near an electrode interface: In the work of Kohler et al.[58] dicyanamide was found to strongly passivate the surface of copper. Additional results regarding the adsorption of molecules at an electrified interface were obtained in potential-dependent spectroscopic experiments for molecules containing C≡N moieties. Molecules such as benzonitrile, probed with electrochemically modulated infrared spectroelectrochemistry (EMIRS),[59] cyanide ion, probed with Fourier transform infrared reflection absorption (FT IRRAS),[60] and ferricyanide, probed with SNIFTIRS,[61] were investigated. In most cases, the C≡N group is shown to strongly adsorb to the metal electrode surface through the nitrile nitrogen atom and increase the coverage at more positive potentials. However, other results may suggest an adsorption through the amide nitrogen, since it was also demonstrated that dicyanamide may coordinate to transition metals in a variety of modes, for example, through one nitrile nitrogen, an end-to-end bridge through two nitrile nitrogens, an amide nitrogen, or combinations of those.[62−67] Nevertheless, the SFG spectroscopy results cannot discriminate between a coordination mode involving the two nitrile nitrogens or the amide nitrogen, since both configurations would give rise to a sum frequency signal. Both configurations are in accordance with the C_2 symmetry axis being aligned with the surface normal, as stated by the spectroscopic analysis. The ppp spectra show similar characteristics regarding the symmetric stretch vibration dip at 2180 cm^{-1}, whose amplitude appears to strongly increase with potential.

The ratio of the amplitudes of the antisymmetric peak and the combination band (marked with asterisks in Figures 9 and 10), which are believed to have a contribution from the liquid−CaF_2 interface, remains approximately the same. These vibrations are therefore not reliable for orientation analysis.

Regarding the C−H vibrations, the ratio of the symmetric methylene stretch (at 2850 cm^{-1}) to the symmetric methyl stretch (at 2879 cm^{-1}) in the ssp spectra slightly diminishes as the potential becomes more positive, suggesting a small increase in the ordering of the alkyl chains. The symmetric stretch ring mode vibration arising from the C_4 and C_5 carbons appears to be more intense at positive potentials, suggesting that the ring is being repelled from the platinum surface and tilting toward the normal, i.e., assuming a vertical position. This outcome is similar to the results of Lipkowski et al.[68] concerning the orientation of pyridine at the surface of gold using SNIFTIRS, where the tilt of the ring appears to be bonded to the metal through the nitrogen atom in a roughly vertical position. In that investigation, at small electric fields, the film of adsorbed molecules is less rigid and shows a waving motion, but as the electric field becomes large, the motion is restrained and the molecules seem to freeze in the vertical position.[68]

Moreover, the fact that the increase of ordering of the alkyl chains is proportional to the charge becoming more positive with respect to the PZC suggests that the cation does not leave the surface completely, but rather tilts as a result of the charge repellence to allow for the dicyanamide adsorption. The work of Bozzini et al. appears to support a coadsorption of ions at the surface of gold(111), where strongly bound cyanide ions do not seem to be affected by the presence of coadsorbed cetylpyridinium cations.[56]

It is nevertheless important to state that the changes in orientation of the molecules in the multilayer of adsorbed ions, which are believed to take place in the system, cannot be known with precision. Moreover, they are conceived as average orientations with respect to the metallic electrode surface. Therefore, the orientation is only qualitatively analyzed.

Conclusions

The platinum liquid interface for [BMIM][DCA] was investigated using differential capacitance measurements and SFG. The cation and the anion were probed at two different vibrational frequency ranges that correspond to the C−H stretch vibrations and the C≡N stretch vibrations. The SFG spectra suggest that the imidazolium ring in the cation tends to lie flat at the surface of the electrode at negative potentials but is repelled at positive ones. The anion seems to be strongly adsorbed at the surface of the platinum at more positive potentials with its C_2 axis aligned with the surface normal. The differential capacitance measurement shows a PZC at approximately −315 mV versus the Ag quasi-reference electrode and a double-layer thickness of ∼25 Å.

Acknowledgment. We are grateful for support from the Welch Foundation (Grant E1531). We also thank Cyré Kalu of the University of Houston for careful editing of this paper.

References and Notes

(1) Buzzeo, M. C.; Evans, R. G.; Compton, R. G. *Chem. Phys. Chem.* **2004**, *5*, 1106.
(2) Welton, T. *Chem. Rev.* **1999**, *99*, 2071.
(3) Sun, J.; Forsyth, M.; MacFarlane, D. R. *J. Phys. Chem. B* **1998**, *102*, 8858.
(4) Golding, J.; Forsyth, S.; MacFarlane, D. R.; Forsyth, M.; Deacon, G. B. *Green Chem.* **2002**, *4*, 223.
(5) Dupont, J.; de Souza, R. F.; Suarez, P. A. Z. *Chem. Rev* **2002**, *102*, 3667.
(6) *Ionic Liquids in Synthesis*; Wasserscheid, P., Welton, T., Eds.; Wiley-VCH: New York, 2003.
(7) *Ionic Liquids*; Inman, D., Lovering, D. G., Eds.; Plenum Press: New York, 1981.
(8) MacFarlane, D. R.; Golding, J.; Forsyth, S.; Forsyth, M.; Deacon, G. B. *Chem. Commun.* **2001**, 1430.
(9) MacFarlane, D. R.; Forsyth, S. A.; Golding, J.; Deacon, G. B. *Green Chem.* **2002**, *4*, 223.
(10) Bloom, H. *The Chemistry of Molten Salts*; W. A. Benjamin Inc.: New York, 1967.
(11) Williams, D. B.; Stoll, M. E.; Scott, B. L.; Costa, D. A.; Oldham, W. J., Jr. *Chem. Commun.* **2005**, 1438.
(12) Sun, J.; MacFarlane, D. R.; Forsyth, M. *Ionics* **1997**, *3*, 356.
(13) Matsumoto, H.; Yanagida, M.; Tanimoto, K.; Nomura, M.; Kitagawa, Y.; Miyasaki, Y. *Chem. Lett.* **2000**, 922.
(14) Matsumoto, H.; Kageyama, H.; Miyasaki, Y. *Chem. Lett.* **2001**, 182.
(15) Matsumoto, H.; Kageyama, H.; Miyasaki, Y. *Chem. Commun.* **2002**, 1726.

(16) Wang, P.; Zakeeruddin, S. M.; Moser, J.-E.; Gratzel, M. *J. Phys. Chem. B* **2003**, *107*, 13280.
(17) Schlueter, J. A.; Geiser, U.; Manson, J. L. *J. Phys. IV* **2004**, *114*, 475.
(18) Graves, A. D. *J. Electroanal. Chem.* **1970**, *25*, 349.
(19) Nanjundiah, C.; McDevitt, S. F.; Koch, V. R. *J. Electrochem. Soc.* **1997**, *144*, 3392.
(20) Gale, R. J.; Osteryoung, R. A. *Electrochim. Acta* **1980**, *25*, 1527.
(21) Devanathan, M. A. V.; Tilak B. V. K. S. R. A. *Chem. Rev.* **1965**, *65*, 635.
(22) Kisza, A. *J. Electroanal. Chem.* **2002**, *534*, 99.
(23) Rivera-Rubero, S.; Baldelli, S. *J. Phys. Chem. B* **2004**, *108*, 15133.
(24) Grahame, D. C. *Chem. Rev.* **1947**, *41*, 441.
(25) *Comprehensive treatise of electrochemistry*; Conway, B. E., Bockris, J. O., Yeager, E., Khan, S. U., White, R. E., Eds.; Plenum Press: New York, 1983; Vol. 7.
(26) Bard, A. J.; Faulkner, L. R. *Electrochemical methods*, 2nd ed.; John Wiley and Sons: New York, 2001.
(27) Wakai, C.; Oleinikova, A.; Ott, M.; Weingartner, H. *J. Phys. Chem. B* **2005**, *109*, 17028.
(28) Sotnikov, A. I.; Esin, O. A. Physical Chemistry and Electrochemistry of Molten Salts and Slags. 3rd All Soviet Conference, Leningrad, 1966.
(29) Shen, Y. R. *The Principles of Nonlinear Optics*; John Wiley and Sons: New York, Chichester, Brisbane, Toronto, Singapore, 1984.
(30) Buck, M.; Himmelhaus, M. *J. Vac. Sci. Technol., A* **2001**, *19*, 2717.
(31) Bloembergen, N. *Nonlinear Optics*; W. A. Benjamin Inc.: New York, Amsterdam, 1965.
(32) *Laser Spectroscopy and Photochemistry on Metal Surfaces*; Dai, H.-L., Ho, W., Eds.; World Scientific: Singapore, 1995; Vol. 5.
(33) Bonhote, P.; Dias, A.-P.; Papageorgiou, N.; Kalayasundaram, K.; Gratzel, M. *Inorg. Chem.* **1996**, *35*, 1168.
(34) Hultgren, V. M.; Mariotti, A. W. A.; Bond, A. M.; Wedd, A. G. *Anal. Chem.* **2002**, *74*, 3151.
(35) Zhang, J.; Bond, A. M. *Anal. Chem.* **2003**, *75*, 2694.
(36) Matsumiya, M.; Terazono, M.; Tokuraku, K. *Electrochim. Acta* **2006**, *51*, 1178.
(37) Baldelli, S.; Mailhot, G.; Ross, P.; Shen, Y.-R.; Somorjai, G. A. *J. Phys. Chem. B* **2001**, *105*, 654.
(38) Hsu, C. H.; Mansfeld, F. *Corrosion* **2001**, *57*, 747.
(39) Bockris, J. O. M.; Reddy A. K. N.; Gamboa-Aldeco, M. *Modern electrochemistry: Fundamentals of Electrodics*, 2nd ed.; Kluwer Academic/Plenum Publishers: New York, 2000; Vol. 2A.
(40) Dahl, K.; Sando, G. M.; Fox, D. M.; Sutto, T. E.; Owrutsky, J. C. *J. Chem. Phys.* **2005**, *123*, 084504.
(41) Lotsch, B. V.; Senker, J.; Kockelmann, W.; Schnick, W. *J. Solid State Chem.* **2003**, *176*, 180.
(42) Snyder, R. G. *J. Chem. Phys.* **1965**, *42*, 1744.
(43) Snyder, R. G.; Strauss, H. L.; Elliger, C. A. *J. Phys. Chem.* **1982**, *86*, 5145.
(44) MacPhail, R. A.; Strauss, H. L.; Snyder, R. G.; Elliger, C. A. *J. Phys. Chem.* **1984**, *88*, 334.
(45) Dieter, K. M.; Dymek, C. J. Jr.; Heimer, N. E.; Rovang, J. W.; Wilkes, J. S. *J. Am. Chem. Soc.* **1988**, *110*, 2722.
(46) Carter, D. A.; Pemberton, J. E. *J. Raman Spectrosc.* **1997**, *28*, 939.
(47) Carter, D. A.; Pemberton, J. E.; Woelfel, K. J. *J. Phys. Chem. B* **1998**, *102*, 9870.
(48) Bockris J. O'M., K., S. U. M. *Surface electrochemistry. A molecular level approach*; Plenum Press: New York, London, 1993.
(49) Baldelli, S. *J. Phys. Chem. B* **2005**, *109*, 13049.
(50) Radom, L.; Riggs, N. V. *Aust. J. Chem.* **1981**, *34*, 7.
(51) Bondino, F.; Baraldi, A.; Over, H.; Comelli, G.; Lacovig, P.; Lizzit, S.; Paolucci, G.; Rosei, R. *Phys. Rev. B* **2001**, *64*, 085422.
(52) Bizzotto, D.; Lipkowsky, J. *J. Electroanal. Chem.* **1996**, *409*, 33.
(53) Sotiropoulos, S.; Avranas, A.; Papadopoulos, N. *Langmuir* **1997**, *13*, 7230.
(54) Tadjeddine, A.; Guyot-Sionnest, P. *Electrochim. Acta* **1991**, *36*, 1849.
(55) Friedrich, K. A.; Daum, W.; Klunker, C.; Knabben, D.; Stimming, U.; Ibach, H. *Surf. Sci.* **1995**, *335*, 315.
(56) Bozzini, B.; Mele, C.; Fanigliulo, A.; Busson, B.; Vidal, F.; Tadjeddine, A. *J. Electroanal. Chem.* **2004**, *574*, 85.
(57) Baldelli, S.; Mailhot, G.; Ross, P. N.; Somorjai, G. A. *J. Am. Chem. Soc.* **2001**, *123*, 7697.
(58) Kohler, J. M.; Kohler, H. *Z. Anorg. Allg. Chem.* **1987**, *555*, 161.
(59) *Electroanalytical Chemistry*; Bard, A. J., Ed.; Marcel Dekker: New York, 1986; Vol. 14.
(60) Kunimatsu, K.; Seki, H.; Golden, W. G.; Gordon, J. G., II; Philpott, M. R. *Langmuir* **1988**, *4*, 337.
(61) Pons, S.; Datta, M.; McAleer, J. F.; Hinman, A. S. *J. Electroanal. Chem.* **1984**, *160*, 369.
(62) Karmakar, R.; Choudhury, C. R.; Hughes, D. L.; Yap, G. P. A.; Salah El Fallah, M.; Desplanches, C.; Sutter, J.-P.; Mitra, S. *Inorg. Chim. Acta* **2006**, *359*, 1184.
(63) Potocnak, I.; Dunaj-Jurco, M.; Miklos, D.; Kabesova, M.; Jager, L. *Acta Crystallogr.* **1995**, *C51*, 600.
(64) Marshall, S. R.; Incarvito, C. D.; Shum, W. W.; Rheingold, A. L.; Miller, J. S. *Chem. Commun.* **2002**, 3006.
(65) Batten, S. R.; Jensen, P.; Kepert, C. J.; Kurmoo, M.; Moubaraki, B.; Murray, K. S.; Price, D. J. *J. Chem. Soc., Dalton Trans.* **1999**, 2987.
(66) Batten, S. R.; Murray, K. S. *Coord. Chem. Rev.* **2003**, *246*, 103.
(67) Kohler, H.; Wusterhausen, H.; Jeschke, M.; Kolbe, A. *Z. Anorg. Allg. Chem.* **1987**, *547*, 69.
(68) Li, N.; Zamlynny, V.; Lipkowsky, J.; Henglein, F.; Pettinger, B. *J. Electroanal. Chem.* **2002**, *524*−*525*, 43.